



# Electronic structure, phonon spectra and electron-phonon interaction in $\text{TiB}_2$ and $\text{ZrB}_2$

S.M. Sichkar<sup>1</sup>, V.N. Antonov<sup>1,2</sup>, and V.P. Antropov<sup>2</sup>

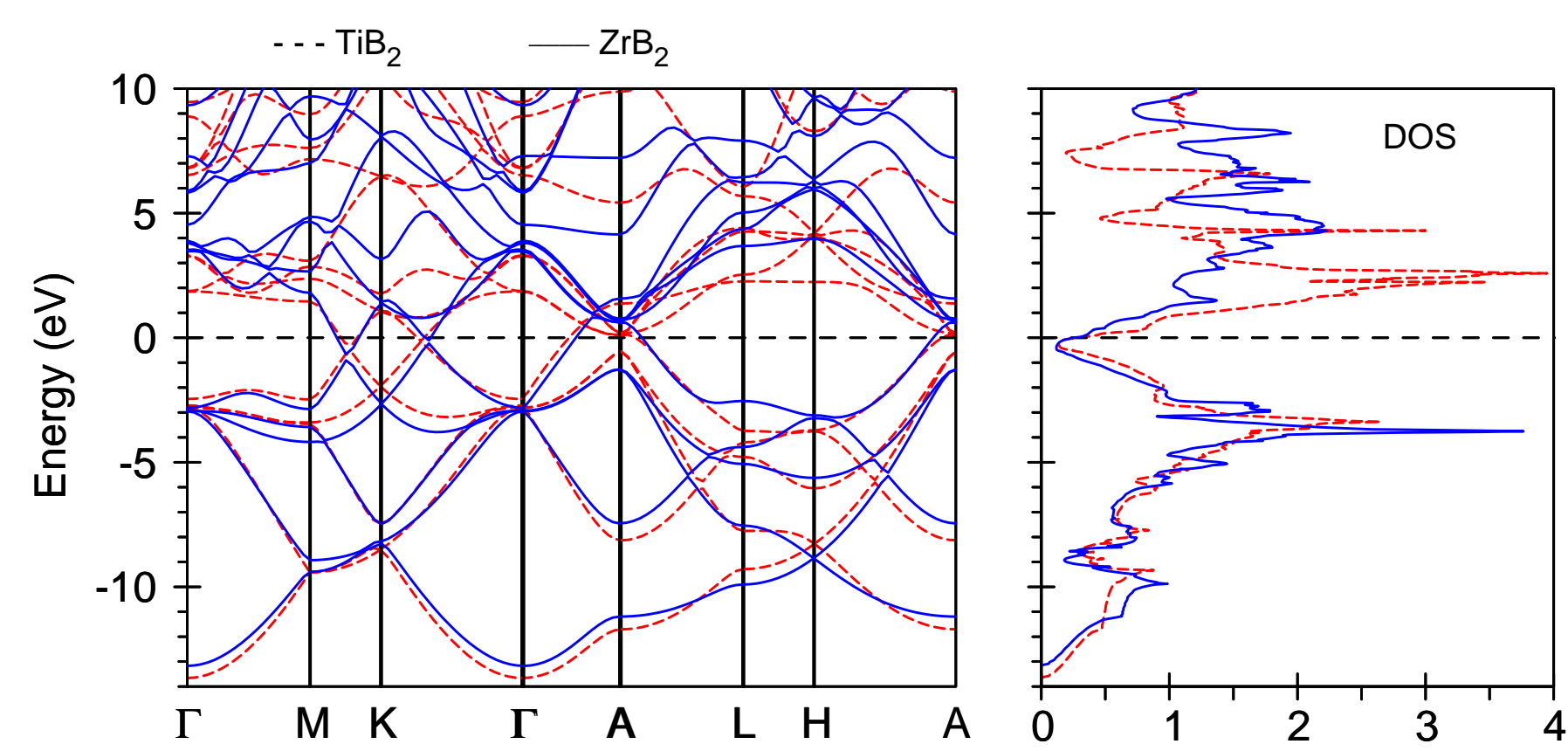
<sup>1</sup>*Institute of Metal Physics, 36 Vernadsky Street, 03680 Kiev-142, Ukraine*

<sup>2</sup>*Ames Laboratory, U.S. Department of Energy, Ames, Iowa 50011, USA*

## Motivations

- The discovery of superconductivity in  $\text{MgB}_2$  at 39 K by Akimitsu [1] has led to booming activity in the physics community and activated a search for superconductivity in other diborides. Natural candidates for this search are  $\text{AB}_2$ -type light metal diborides ( $A = \text{Li, Be, Al}$ ). However, up to now superconductivity has not been reported in the majority of these compounds. According to Ref. [2] no superconducting transition down to 0.42 K has been observed in powders of diborides of transition metals ( $A = \text{Ti, Zr, Hf, V, Ta, Cr, Mo, U}$ ). Only  $\text{NbB}_2$  is expected to superconduct with a rather low transition temperature ( $< 1$  K). Finally, the reported  $T_c=7$  K in  $\text{ZrB}_2$  [3] encourages further studies of these diborides.
- The electronic structure, optical and x-ray absorption spectra, angle dependence of the cyclotron masses and extremal cross sections of the Fermi surface, phonon spectra, electron-phonon Eliashberg and transport spectral functions, temperature dependence of electrical resistivity of the  $\text{MB}_2$  ( $M=\text{Ti}$  and  $\text{Zr}$ ) diborides were investigated from first principles using the fully relativistic and full potential linear muffin-tin orbital methods. The calculations of the dynamic matrix were carried out within the framework of the linear response theory.

## Energy band structure



Energy band structure of  $\text{TiB}_2$  and  $\text{ZrB}_2$

## Optical spectra

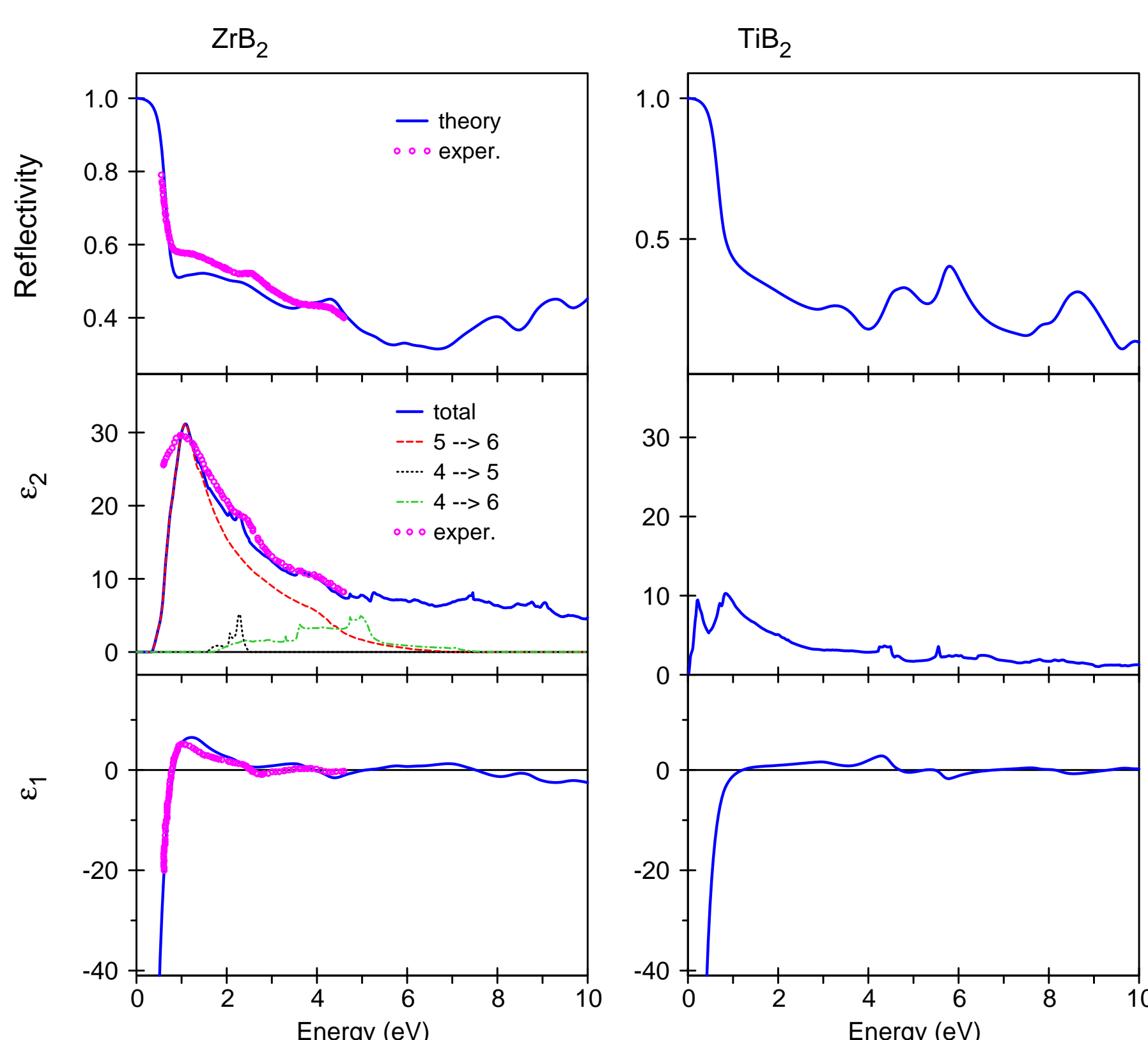
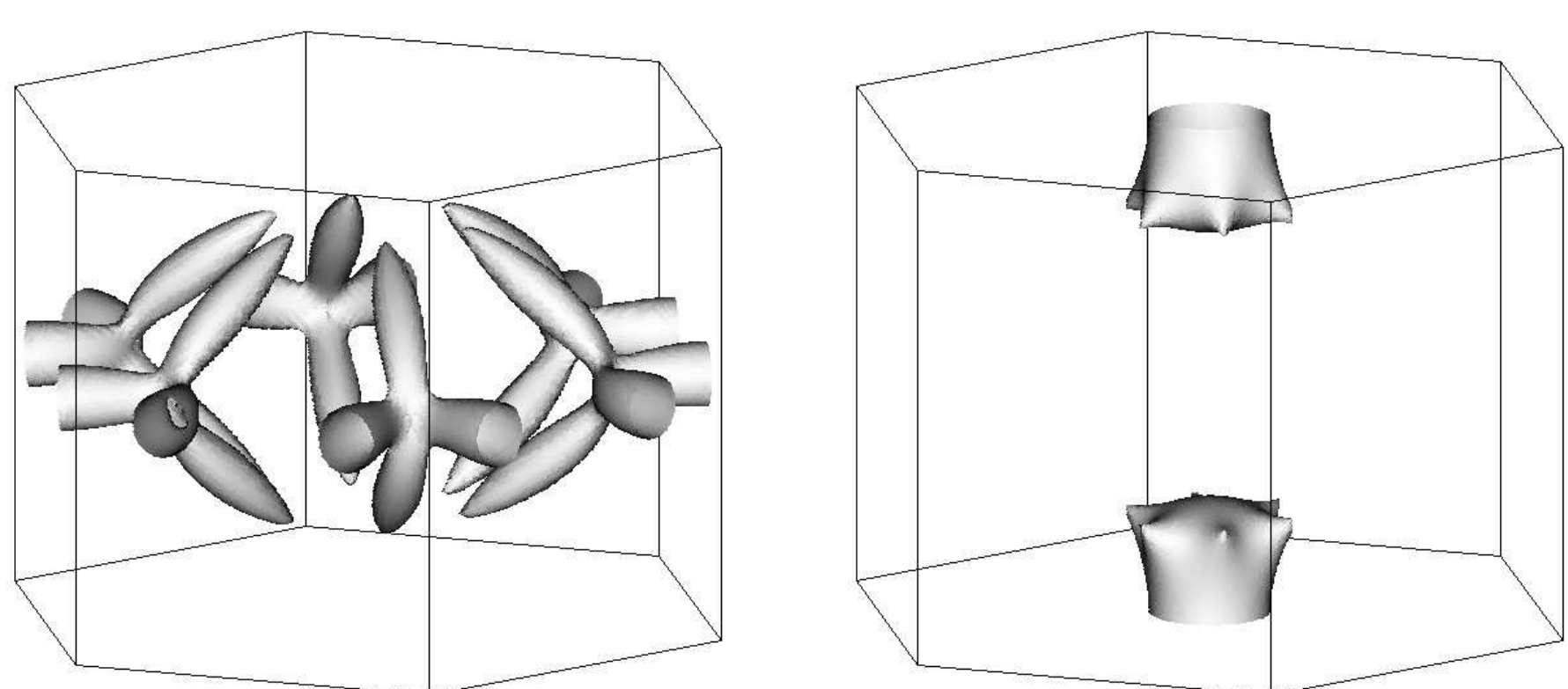


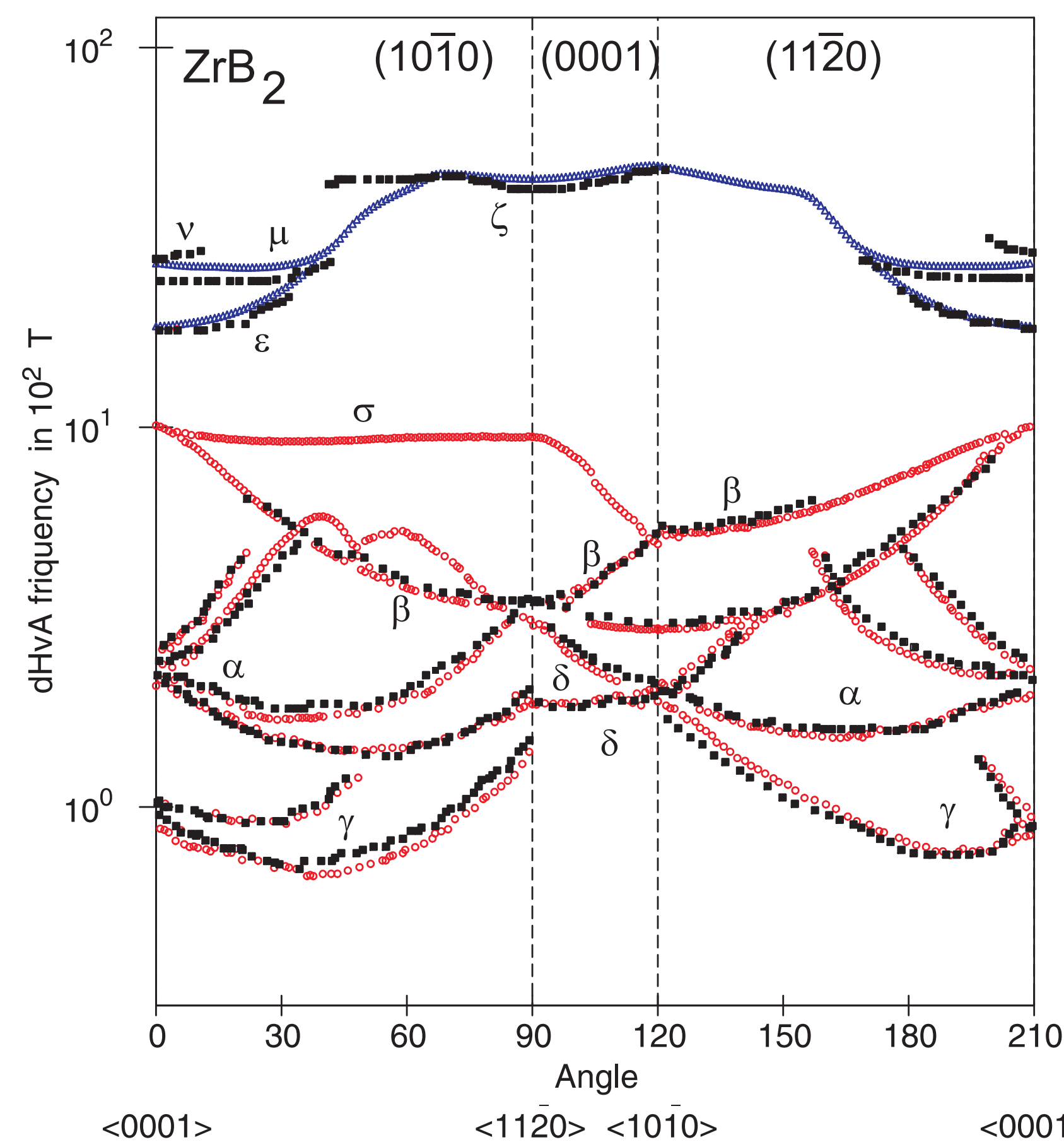
Figure presents the theoretically calculated and experimentally measured [4] optical reflectivity spectra  $R(\omega)$  as well as dielectric constants  $\epsilon_1(\omega)$  and  $\epsilon_2(\omega)$  for  $\text{ZrB}_2$  and  $\text{TiB}_2$ . We performed decomposition of the calculated  $\epsilon_2$  spectrum into the contributions arising from separate interband transitions and different places of  $\mathbf{k}$  space. We found that the major peak in the  $\epsilon_2(\omega)$  (around 1 eV) is mostly determined by the  $5 \rightarrow 6$  interband transitions along the  $\Gamma-A$  and  $A-L$  symmetry directions. The shoulder at 2 eV is due to the  $4 \rightarrow 5$  interband transitions around A symmetry point.

## Fermi surface



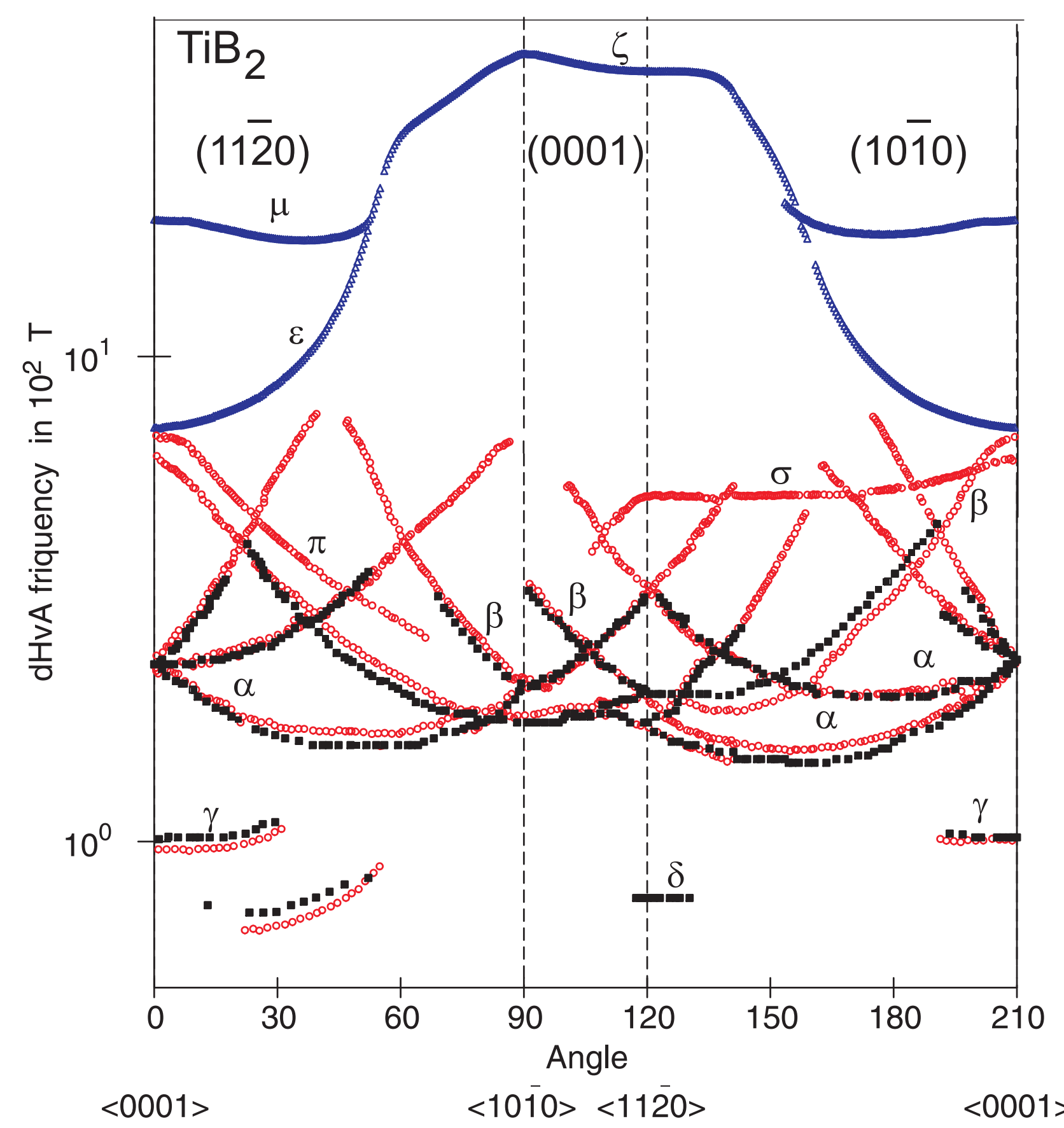
Theoretical calculations show a ring-like electron FS around the  $K$  symmetry point (left panel) and of a wrinkled dumbbell-like hole FS at the A point (right panel) in  $\text{ZrB}_2$  and  $\text{TiB}_2$ . The electron FS and hole FS have threefold and sixfold symmetries, respectively.

## dHvA effect in $\text{ZrB}_2$



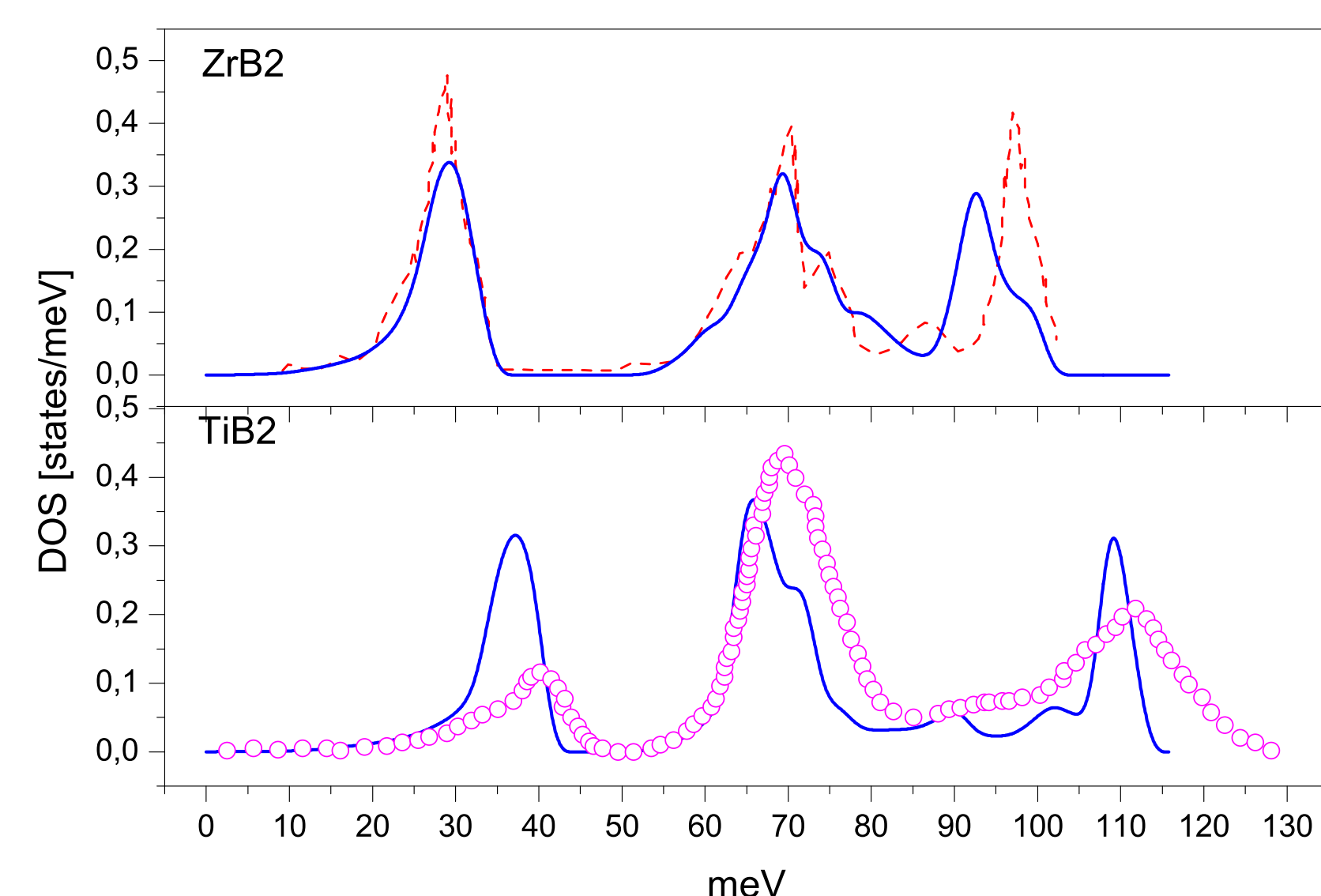
Angular variations of the experimentally measured dHvA frequencies [5] for  $\text{ZrB}_2$  (black squares) in comparison with theory (red and blue circles). The observed frequencies of  $\alpha, \beta, \gamma,$  and  $\delta$  oscillations belong to electron FS around the  $K$  point. The  $\epsilon, \nu, \mu,$  and  $\zeta$  orbits belong to the hole wrinkled dumbbell FS. The theory reasonably well reproduces the frequencies measured experimentally. We discover a new branch  $\sigma$  which belongs to the electron FS around the  $K$  point.

## dHvA effect in $\text{TiB}_2$



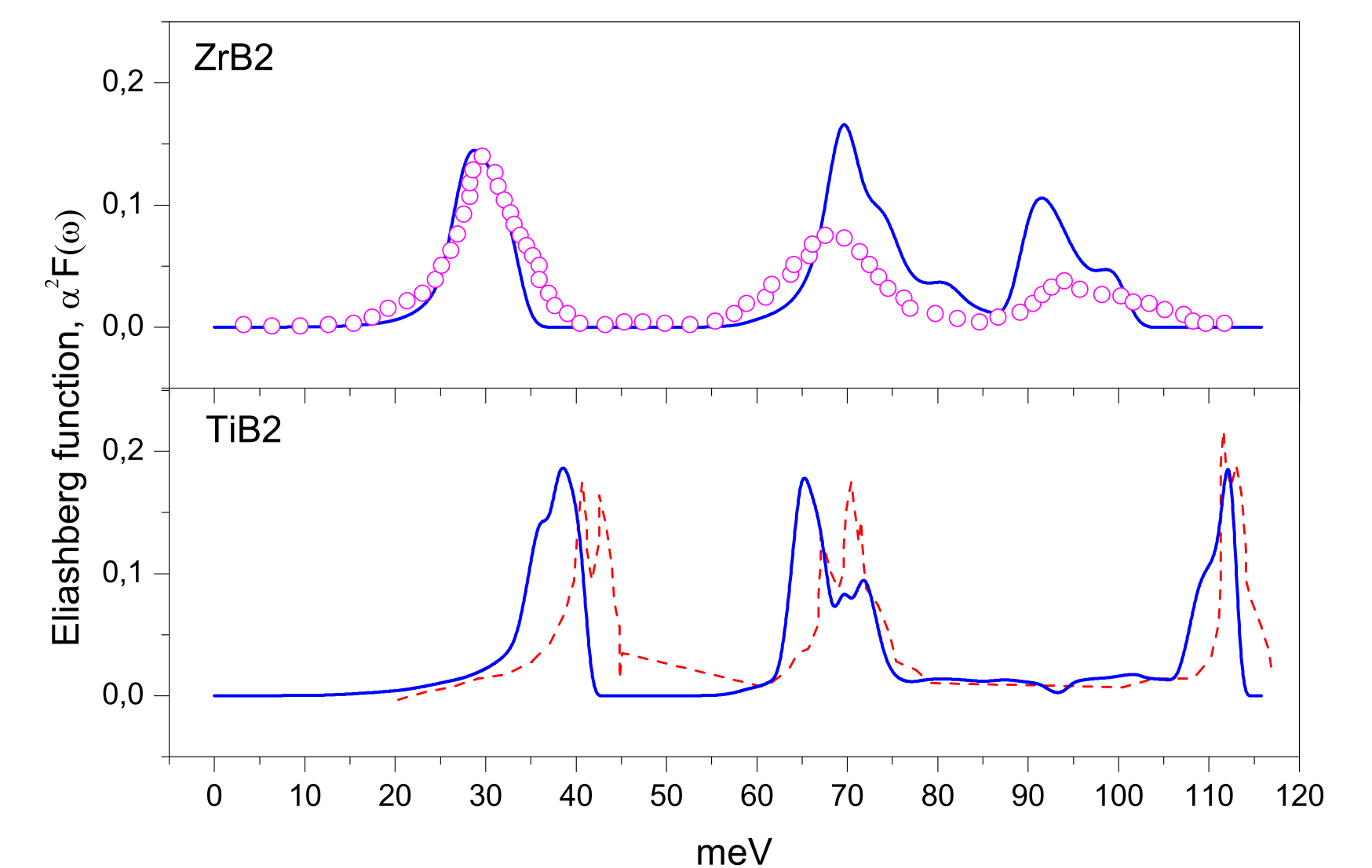
Angular variation of experimentally measured dHvA frequencies in  $\text{TiB}_2$  [6] in comparison with theoretical calculations. The theoretical calculations quite well reproduce the angle dependence of the extremal cross sections for low frequency orbits  $\gamma, \alpha$  and  $\beta$ . Similar to  $\text{ZrB}_2$  we detected theoretically a new branch  $\sigma$  in  $\text{TiB}_2$  which is not observed experimentally. This branch belongs to the electron FS around the  $K$  point. We also find an additional orbit  $\pi$  at the  $(11\bar{2}0)$  plane which is absent in  $\text{ZrB}_2$  and did not detected experimentally. For high frequencies we found the  $\epsilon, \mu$  and  $\zeta$  branches similar to the corresponding orbits in  $\text{ZrB}_2$ . However, these orbits have not been detected in the dHvA experiment. One of the possible reasons for that is the relatively large cyclotron masses for these orbits. We found that the cyclotron masses for the  $\epsilon, \mu,$  and  $\zeta$  orbits in  $\text{TiB}_2$  are much higher than the corresponding orbits in  $\text{ZrB}_2$ . The masses for the low-frequency oscillations  $\alpha, \beta, \gamma$  and  $\delta$  are less than  $0.2m_0$  for  $\text{ZrB}_2$ .

## Phonon DOS



Theoretical phonon density of states (full blue lines) for  $\text{ZrB}_2$  and  $\text{TiB}_2$  and experimentally measured one for  $\text{TiB}_2$  [4] (open circles). Dashed red line presents the calculated phonon DOS of  $\text{ZrB}_2$  by Deligoz *et al.* [8].

## Electron phonon interaction



The theoretically calculated Eliashberg function  $\alpha F(\omega)$  of  $\text{ZrB}_2$  and  $\text{TiB}_2$  (full blue lines) and experimentally measured point contact spectral function [9] (open circles) for  $\text{ZrB}_2$ . Dashed red line presents Eliashberg function of  $\text{TiB}_2$  calculated by Heid *et al.* [10].

## Electrical resistivity

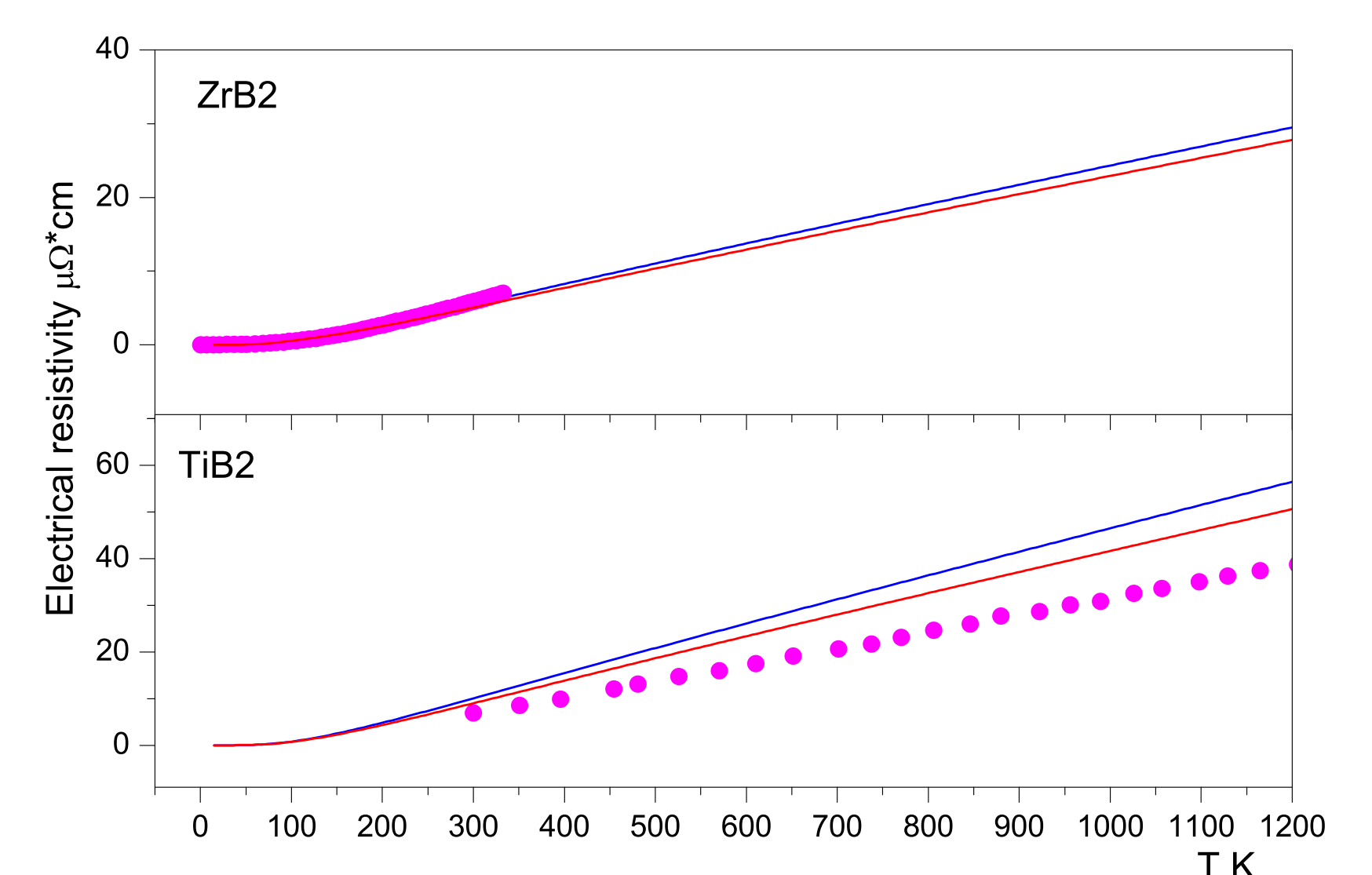


Figure represents the experimental data for mono-crystalline  $\text{ZrB}_2$  (upper panel) and  $\text{TiB}_2$  (lower panel) [11] as well as our calculations. We found that the anisotropy of the electrical resistivity in  $\text{TiB}_2$  (lower panel) is larger than it was in  $\text{ZrB}_2$ . Our theoretical results slightly exceed experimental data, especially at high temperatures. This is due to using in our calculations the lowest-order variational approximation in solution of the Boltzmann equation which gives upper limit for the electrical resistivity.

## Conclusions

- Theory reproduces the experimentally measured dHvA frequencies in both the  $\text{ZrB}_2$  and  $\text{TiB}_2$  reasonably well. We found that masses for low-frequency oscillations  $\alpha, \beta, \gamma,$  and  $\delta$  are less than  $0.2m_0$ . Masses for high-frequency oscillations  $\epsilon, \nu, \mu,$  and  $\zeta$  are large. The cyclotron masses for these orbits in  $\text{TiB}_2$  are much higher than the corresponding orbits in  $\text{ZrB}_2$ . It could be one of the reasons why they have not been observed in the dHvA measurements.
- Calculated phonon spectra and phonon DOSs for both  $\text{ZrB}_2$  and  $\text{TiB}_2$  are in good agreement with experimental results as well as previous calculations. The Eliashberg function of electron-phonon interaction in  $\text{ZrB}_2$  is in good agreement with the experimentally measured point contact spectral function for both the position and the shape of the major peaks. We did not find regions with high electron-phonon interaction or phonon dispersion curves with soft modes in either  $\text{ZrB}_2$  or  $\text{TiB}_2$ . This is in agreement with the fact that no trace of superconductivity was found in these borides. The averaged electron-phonon interaction constant was found to be rather small  $\lambda_{e-ph}=0.14$  and  $0.15$  for  $\text{ZrB}_2$  and  $\text{TiB}_2$ , respectively. We calculated the temperature dependence of the electrical resistivity in  $\text{ZrB}_2$  and  $\text{TiB}_2$  in the lowest-order variational approximation of the Boltzmann equation. We found rather small anisotropical behavior of the electrical resistivity in  $\text{ZrB}_2$  to be in good agreement with experimental observation. We found that the anisotropy of electrical resistivity in  $\text{TiB}_2$  is larger than it is in  $\text{ZrB}_2$ .
- The results are published in: S. M. Sichkar, V. N. Antonov, and V. P. Antropov - Phys. Rev. B **87**, 064305 (2013).

## References

- [1] J. Nagamatsu, N. Nakagawa, T. Muranaka, Y. Zenitani, and J. Akimitsu, Nature (London) **410**, 63 (2001).
- [2] C. Buzea *et al.*, Supercond. Sci. Technol. **14**, R115 (2001).
- [3] V. A. Gasparov *et al.*, JETP Lett. **73**, 532 (2001).
- [4] R. Roucka *et al.*, Solid-State Electron. **52**, 1687 (2008).
- [5] V. B. Pluzhnikov *et al.*, Low Temp. Phys. **33**, 350 (2007).
- [6] T. Tanaka and Y. Ishikawa, J. Phys. C **13**, 6671 (1980).
- [7] R. Heid *et al.*, Phys. Rev. B **67**, 180510(R) (2003).
- [8] E. Deligoz *et al.*, Solid State Commun. **150**, 405 (2010).
- [9] Y. G. Naidyuk *et al.*, Phys. Rev. B **66**, 140301(R) (2002).
- [10] R. Heid *et al.*, Phys. Rev. B **67**, 180510(R) (2003).
- [11] A. D. McLeod *et al.*, J. Am. Ceram. Soc. **67**, 705 (1984).